



RESEARCH LETTER

10.1002/2015GL064250

Key Points:

- A global observations-based Holocene and LGM dust flux data set is presented
- Iron fertilization reduced LGM atmospheric CO₂ levels by 20 ppm
- The new data set is an improvement over currently used simulated dust fluxes from various models

Supporting Information:

- Figure S1
- Figure S2
- Figure S3
- Figure S4
- Figure S5
- Figure S6
- Figure S7
- Figure S8
- Figure S9
- Text S1 and Table S1

Correspondence to:

F. Lambert,
lambert@uc.cl

Citation:

Lambert, F., A. Tagliabue, G. Shaffer, F. Lamy, G. Winckler, L. Farias, L. Gallardo, and R. De Pol-Holz (2015), Dust fluxes and iron fertilization in Holocene and Last Glacial Maximum climates, *Geophys. Res. Lett.*, 42, doi:10.1002/2015GL064250.

Received 18 MAY 2015

Accepted 7 JUL 2015

Accepted article online 14 JUL 2015

Dust fluxes and iron fertilization in Holocene and Last Glacial Maximum climates

Fabrice Lambert^{1,2}, Alessandro Tagliabue³, Gary Shaffer^{4,5,6}, Frank Lamy⁷, Gisela Winckler⁸, Laura Farias⁹, Laura Gallardo², and Ricardo De Pol-Holz⁵

¹Department of Physical Geography, Pontifical Catholic University of Chile, Santiago, Chile, ²Center for Climate and Resilience Research, University of Chile, Santiago, Chile, ³School of Environmental Sciences, University of Liverpool, Liverpool, UK, ⁴Center for Advanced Studies in Arid Zones, La Serena, Chile, ⁵GAI-Antarctica, University of Magallanes, Punta Arenas, Chile, ⁶Niels Bohr Institute, University of Copenhagen, Copenhagen, Denmark, ⁷Alfred Wegener Institute, Helmholtz Centre for Polar and Marine Research, Bremerhaven, Germany, ⁸Lamont-Doherty Earth Observatory, Columbia University, New York, USA, ⁹Department of Oceanography, University of Concepcion, Concepcion, Chile

Abstract Mineral dust aerosols play a major role in present and past climates. To date, we rely on climate models for estimates of dust fluxes to calculate the impact of airborne micronutrients on biogeochemical cycles. Here we provide a new global dust flux data set for Holocene and Last Glacial Maximum (LGM) conditions based on observational data. A comparison with dust flux simulations highlights regional differences between observations and models. By forcing a biogeochemical model with our new data set and using this model's results to guide a millennial-scale Earth System Model simulation, we calculate the impact of enhanced glacial oceanic iron deposition on the LGM-Holocene carbon cycle. On centennial timescales, the higher LGM dust deposition results in a weak reduction of <10 ppm in atmospheric CO₂ due to enhanced efficiency of the biological pump. This is followed by a further ~10 ppm reduction over millennial timescales due to greater carbon burial and carbonate compensation.

1. Introduction

Mineral dust aerosols in the atmosphere affect the climate directly by absorbing and scattering incoming solar and outgoing infrared radiation [Tegen *et al.*, 1996; Sokolik *et al.*, 2001] and indirectly by acting as ice nuclei [Sassen *et al.*, 2003; Lohmann and Feichter, 2005]. The deposition of dust on the Earth's surface also provides the terrestrial biosphere and surface ocean with micronutrients, affecting biogeochemical cycles [Martin *et al.*, 1991; Bristow *et al.*, 2010; Mahowald, 2011]. Early efforts to simulate dust deposition under past climatic conditions were conducted using various global climate models [Mahowald *et al.*, 1999; Werner *et al.*, 2002; Tegen, 2003]. Within the Paleoclimate Modeling Intercomparison Project (PMIP) 2, dust simulations were performed using the CAM3-CCSM3 [Mahowald *et al.* [2006], hereafter CCSM] and SPRINTARS-MIROC3 [Takemura *et al.* [2009], hereafter MIROC] climate models. Recently, the PMIP 3 climate models MIROC-ESM [Watanabe *et al.*, 2011] and MRI-CGCM3 [Yukimoto *et al.* [2012], hereafter MRI] also included dust in their paleoclimatic simulations. However, there are significant differences in dust load and spatial distribution among various dust simulations, even under modern conditions [Huneus *et al.*, 2011].

From an observational perspective, paleoclimatic archives provide us with a record of past variability of dust deposition at specific locations. An extensive amount of Holocene and Last Glacial Maximum (LGM) dust flux measurements were compiled in the DIRTMAP database [Kohfeld and Harrison, 2001; Maher *et al.*, 2010]. These observations have varying analytical uncertainties, and the spatial distribution of the global data set is irregular. Globally, the LGM atmosphere is thought to have contained 3–4 times more dust than during the Holocene [Kohfeld and Harrison, 2001; Maher *et al.*, 2010], which reflects the changes in the tropics, where most of the atmospheric dust is emitted. In remote regions far away from sources, LGM dust deposition has been found to be 2–3 times higher in the tropical and South Pacific [Winckler *et al.*, 2008; Kohfeld *et al.*, 2013; Lamy *et al.*, 2014], ~5 times higher in the South Atlantic [Martínez-García *et al.*, 2009] and 20–30 times higher in polar regions [Steffensen, 1997; Lambert *et al.*, 2008, 2013].

Dustborne iron fertilization of the nutrient-rich Southern Ocean (SO) waters and the subsequent sequestration of carbon in the ocean interior has been proposed as a driver of lower levels of atmospheric CO₂ during glacial periods of the late Pleistocene [Martin *et al.*, 1990]. In certain regions of the world's oceans known as

“High Nutrient Low Chlorophyll” (HNLC) regions, macronutrients like nitrate and phosphate are abundant, but the lack of iron restricts oceanic primary productivity [Martin and Fitzwater, 1988]. It is argued that increased aeolian iron input during the LGM stimulated primary production, thus amplifying the actions of the biological and carbonate pumps that transport carbon down from the ocean surface [Martin, 1990; Martin et al., 1990; Hain et al., 2014]. Artificial iron fertilization experiments have stimulated phytoplankton blooms [e.g., Coale et al., 1996; Boyd et al., 2000, 2007], with more than half of the captured carbon potentially able to sink into the deep ocean [Smetacek et al., 2012]. However, it is unclear how much of the sinking carbon returns to the ocean surface layers [de Baar, 2005]. Studies using paleoclimatic records of high southern latitudes to link dust deposition to marine productivity estimate that increased Last Glacial Maximum (LGM) dust deposition may have contributed up to 40% of the Holocene-LGM difference of 80–100 ppm in the partial pressure of atmospheric CO₂ ($p\text{CO}_2$) [Röthlisberger et al., 2004; Martínez-García et al., 2011; Lambert et al., 2012]. In contrast, many model studies that directly relate the ocean carbon cycles to fluctuations in dust deposition tend to assign a lower significance (<20%) to this phenomenon [Bopp et al., 2003; Ridgwell, 2003; Parekh et al., 2006; Tagliabue et al., 2009, 2014], although these models usually focus on biological productivity over centennial timescales and thereby neglect millennial-scale processes of carbon burial and carbonate compensation.

Here we present a new interpolation of the unevenly spaced Holocene and LGM dust flux measurements compiled in the DIRTMAP database [Kohfeld and Harrison, 2001; Maher et al., 2010] to two global grids. We compare our interpolated dust deposition fields with four climate model simulations of global dust flux to identify regions with large discrepancies. We use our interpolated dust fluxes to force a biogeochemical model and calculate the carbon export impact due to iron fertilization between Holocene and LGM climatic conditions. Together with a long Earth System Model simulation guided by results of the biogeochemical model, we estimate the centennial- and millennial-scale effects of carbon export changes on atmospheric $p\text{CO}_2$ levels.

2. Methods

The spatial distribution of dust flux measurements has greatly improved in recent times, with the third version of the DIRTMAP database including almost twice the number of sites compared to the previous version [Maher et al., 2010]. For this study we used 375 and 311 data points for average Holocene and LGM conditions, respectively, with additional data points not included in DIRTMAP 3 listed in Table S1 in the supporting information (SI). The data locations are sufficiently well distributed to perform a global interpolation on a T42 (128 longitude \times 64 latitude) grid. At first order, the aerosol concentration in an air parcel decreases at an exponential rate with distance from the source [Hansson, 1994; Ruth et al., 2003; Fischer et al., 2007]. We extend this exponential relationship with distance to produce deposition fluxes, assuming in effect constant deposition velocities. This assumption is valid as we are considering multiyear average Holocene and LGM values and not seasonal variations and as dust flux is lognormally distributed on a large scale in all climate models (SI Figure S3). We do not account for the fact that the dry deposition velocity changes due to varying surface roughness; however, this is justified by the fact that in the majority of the world and particularly over land, wet deposition dominates [Mahowald et al., 2006; Takemura et al., 2009]. Large-scale precipitation and wind direction patterns result in directional variance that is around 4 times higher in the north-south direction than in the east-west direction. This anisotropy of the field results from the preferential zonal transport of dust by the main wind currents and was addressed in the directional semivariogram of the interpolation procedure (see SI). Thus, we interpolated the logarithmic values of the measured dust fluxes using a Kriging algorithm [Cressie, 1991] (Figure 1). For loess data that usually contain a significant fraction of large dust particles that do not travel far, we used the PM10 (particle diameter <10 μm) fraction, whereas total dust deposition measurements from ice cores and marine sediments were considered as representing long-range transport. This primary stage is similar to the method used previously [Lambert et al., 2013]. Here we additionally corrected the variogram for the difference in distance represented by 1° of longitude at low and high latitudes (see SI), thus, producing a global data set of yearly average dust fluxes for both Holocene and LGM conditions. The distribution of the original dust flux measurements, the interpolation, and the simulations of the four models we used are compared in SI Figure S3 and show the spatial lognormality of dust deposition. To force the biogeochemistry

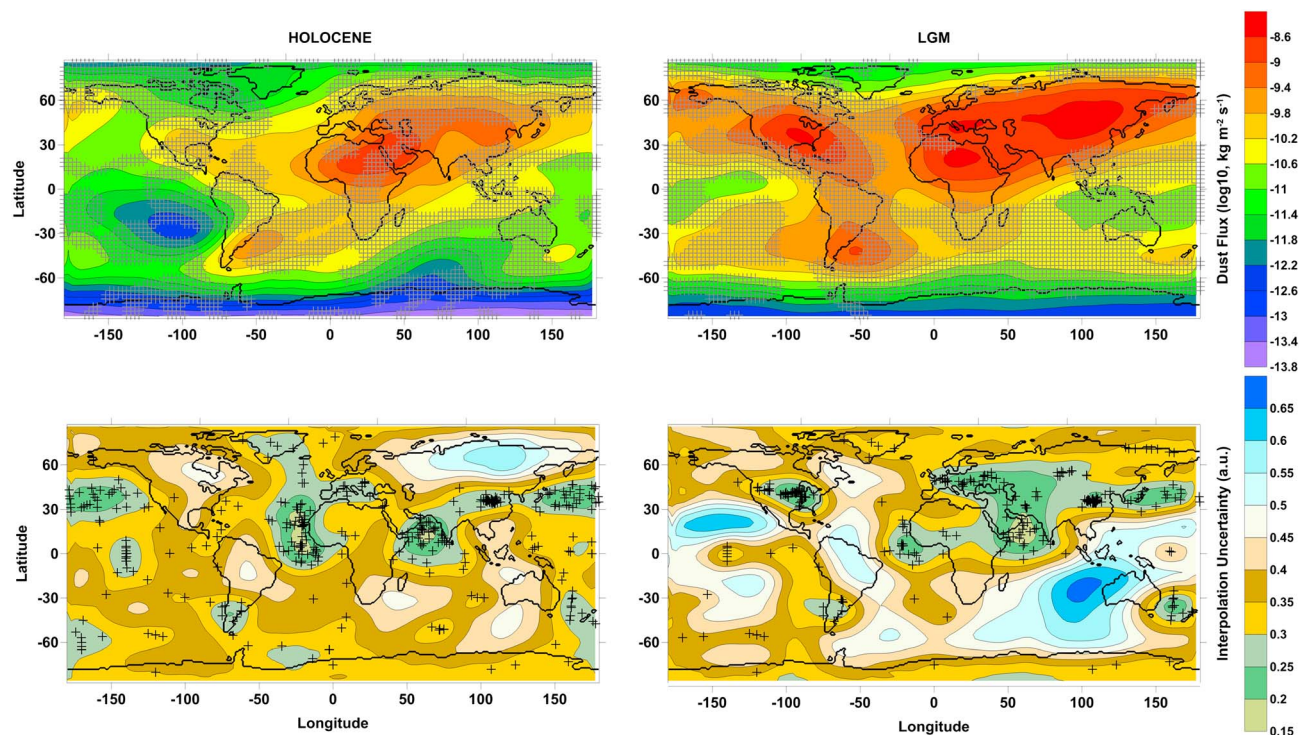


Figure 1. (top row) Global maps of interpolated dust flux for Holocene and LGM conditions. Nonshaded and shaded areas show regions with interpolation uncertainty smaller and higher than the global mean (Holocene: 0.35, LGM: 0.39), respectively. (bottom row) Uncertainty of the interpolation due to the spatial density of dust flux measurements. Data points are indicated with a cross.

model, a monthly component was added by applying the ensemble median of the monthly variations around the yearly mean from the four climate models at each grid cell.

The interpolated global dust flux grid was used to force the biogeochemical model NEMO-PISCES [Tagliabue *et al.*, 2014]. Although the iron fraction of dust and the iron solubility are spatially and temporally variable [Schroth *et al.*, 2009], we kept these values constant as in previous simulations [Tagliabue *et al.*, 2014] because of the lack of available observations. PISCES is a relatively complex ocean biogeochemical model that considers two phytoplankton size classes, two zooplankton grazers, two particle size classes, and five nutrients (nitrate, phosphate, silicic acid, ammonium, and iron). The iron cycle in PISCES accounts for organic speciation, scavenging, and its variable biological uptake and considers iron sources from dust, rivers, sediments, and hydrothermal vents [Tagliabue *et al.*, 2014]. The enhancement of nitrogen fixation through additional dust input in tropical oceans [Mills *et al.*, 2004] is present in PISCES simulations. We conducted simulations of 500 years where the dust field was replaced by the LGM and Holocene fields produced in this study. By coupling a well-mixed atmospheric reservoir, we were able to determine the influence of dust variations on atmospheric $p\text{CO}_2$ levels on centennial scales. Lastly, we conducted a 50,000 year simulation with the Danish Center for Earth System Science (DCESS) Earth System Model [Shaffer *et al.*, 2008; Zickfeld *et al.*, 2013] using the relative enhancement of high-latitude export production found in the shorter PISCES simulations. With its relatively sophisticated ocean sediment module, the DCESS model allows us to estimate the millennial-scale CO_2 effects of iron fertilization from carbon burial and carbonate compensation.

3. Results and Discussion

On average, we find the interpolated global LGM dust flux to be about 4 times higher than during the Holocene (Figure 1, top row). This is in the upper range of previous estimates based on observational data [Kohfeld and Harrison, 2001; Maher *et al.*, 2010] and slightly higher than model results [Werner *et al.*, 2002; Mahowald *et al.*, 2006; Takemura *et al.*, 2009; Watanabe *et al.*, 2011; Yukimoto *et al.*, 2012], which may reflect the recognized underestimation of dust over land in models [Maher *et al.*, 2010]. The uncertainty of

the interpolation is indicated in Figure 1 (bottom row). By definition and within the uncertainty of the observations (which the models have to deal with as well for their validation), the interpolation is a more trustworthy estimate for dust fluxes than the models in the vicinity of measurement points. In Figure 1 (top row) the nonshaded areas correspond to data where the uncertainty is smaller than its global mean (i.e., the more trustworthy half), whereas the shaded regions correspond to uncertainties higher than the mean.

North and South American sources appear particularly more potent in the interpolation during the LGM than during the Holocene, something which is generally difficult to reproduce in models [Mahowald *et al.*, 2006; Takemura *et al.*, 2009; Watanabe *et al.*, 2011; Yukimoto *et al.*, 2012]. A large part of the North Atlantic LGM dust deposition appears to originate from sources in North America and North Africa (Figure 1). Although dust in Greenland ice cores has traditionally been considered to originate in Asia [Biscaye *et al.*, 1997; Svensson *et al.*, 2000], its isotopic signature remains ambiguous [Burton *et al.*, 2007; Aleinikoff *et al.*, 2008] and few LGM reference samples have been measured. In our interpolation, Siberian and Alaskan LGM dust sources were very strong and may have also been potential contributors to Greenland dust. In the Southern Hemisphere, extremely low Holocene dust fluxes are observed in the subtropical South Pacific gyre, a situation that persists today in one of the most oligotrophic and iron-limited regions of the world [Blain *et al.*, 2008]. This characteristic appears not to have been present during the LGM, though, possibly due to enhanced dust transport from Australasia, but maybe also westward from the South American continent. The southern part of the LGM dust “plume” west of South America (Figure 1) may be an interpolation artifact, as it goes against the prevailing westerly winds and there are few local measurements to constrain these values. In midlatitudes, however, aerosol incursions from coastal areas into these waters have been documented under modern conditions [Huneeus *et al.*, 2006; Saide *et al.*, 2012] and one could imagine a scenario where dust from strong LGM sources in northern Chile was picked up by coastal lows and transported far into the Pacific via the Pacific subtropical high. In addition, model results also show a large incursion of South American dust into the southeast Pacific, even in the southern part of South America during LGM conditions [Albani *et al.*, 2014]. Although the effect of Australian and New Zealand sources are visible downwind of the source regions into the SW Pacific, the lack of terrestrial observational data from Australia results in a probable underestimation of dust fluxes over that continent in our data set. The uncertainty of the interpolation process (Figure 1, bottom row) is a good indicator of where the interpolation is robust and where dust flux measurements are sparse and new measurements are most needed to better constrain the dust fields. The sparsity of terrestrial data available for the Holocene is due to the fact that loess deposition is largely limited to glacial periods. New observations from peat bogs [Kylander *et al.*, 2013] in Siberia, North America, and South America are expected to fill this gap. The regions with largest uncertainty during the LGM are now located in the Indian Ocean and the oceanic subtropical Pacific.

In Figure 2 we compare the spatial distribution of our dust flux interpolation with simulated output from the four climate models (CCSM, MIROC, MIROC-ESM, and MRI). To account for biases in the interpolation and the climate models, we have standardized each data set by removing the mean and dividing by the standard deviation of the logarithms of the dust fluxes (dust fluxes are spatially lognormally distributed, see SI Figure S3). In Holocene conditions these include large parts of the world’s oceans, as well as the East Asian dust source regions. During the LGM there is a high confidence level for all major dust source regions except for Australia. Based on these results we suggest that dust models generally overestimate LGM dust deposition over West Africa and underestimate it over North America. All but the CCSM also underestimate Siberian LGM sources. Both MIROC models underestimate LGM South American sources. Finally, there are large discrepancies between all model outputs and the interpolation in the HNLC regions of the oceans. The South Pacific dust deposition especially seems to be underestimated in all models over both periods (see also SI Figures S4 to S7).

To evaluate the initial impact of dust fluxes on the ocean carbon cycle, we forced the PISCES model with our interpolated dust deposition fields, providing estimates of oceanic carbon export for both Holocene and LGM conditions. During both periods, the main HNLC regions (as illustrated by high simulated surface nitrate concentrations, Figure 3a, left column) are the SO and the subarctic North Pacific. Carbon export during both periods is highest where there is a substantial supply of nutrients to surface waters (Figure 3a, right column). During the LGM, the additional iron input from aeolian dust increases surface nutrient consumption and reduces preformed nutrient concentrations in line with increased carbon export by the more efficient biological pump in iron-limited regions, i.e., those with excess nitrate, in the Holocene (Figure 3b). High rates

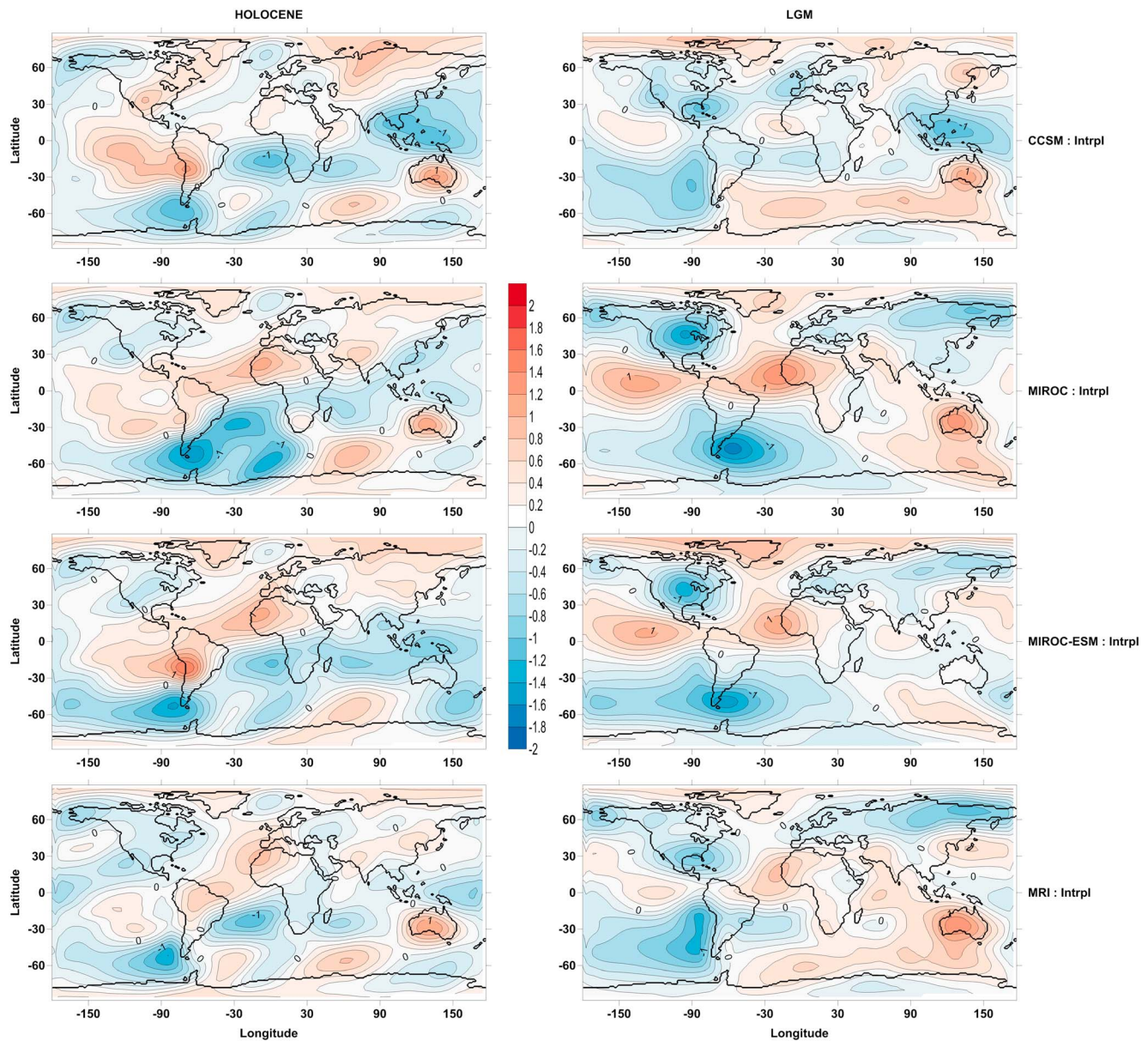


Figure 2. Ratio of standardized global dust fluxes from various climate models with the standardized interpolated dust fluxes. The color scale shows powers of 10.

of LGM dust deposition in the North Atlantic also increased carbon export in this seasonally iron-limited region [Nielsdóttir *et al.*, 2009]. The SO response is heterogeneous, with decreased nitrate and increased carbon export downwind of the South American and Australasian LGM sources, consistent with recent observations [Anderson *et al.*, 2014; Lamy *et al.*, 2014; Martínez-García *et al.*, 2014]. However, there is little iron fertilization from LGM dust in the Antarctic sector of the SO, despite a large reservoir of available macronutrients. Our model results suggest that iron limitation in the Antarctic SO did not change markedly between Holocene and LGM scenarios, due to the preferential zonal transport of dust via the westerlies, which results in very low rates of iron deposition at high southerly latitudes under both Holocene and LGM conditions (see Figure 4 and SI Figure S8).

Previous studies have suggested that about half the observed Holocene-LGM difference of 80–100 ppm in the atmospheric $p\text{CO}_2$ concentrations were due to a stronger stratification of the Antarctic SO and associated carbon buildup in the deep ocean, isolating CO_2 from the atmosphere [Francois *et al.*, 1997; Fischer *et al.*, 2010; Hain *et al.*, 2010; Sigman *et al.*, 2010; Martínez-Botí *et al.*, 2015]. Much of the remaining

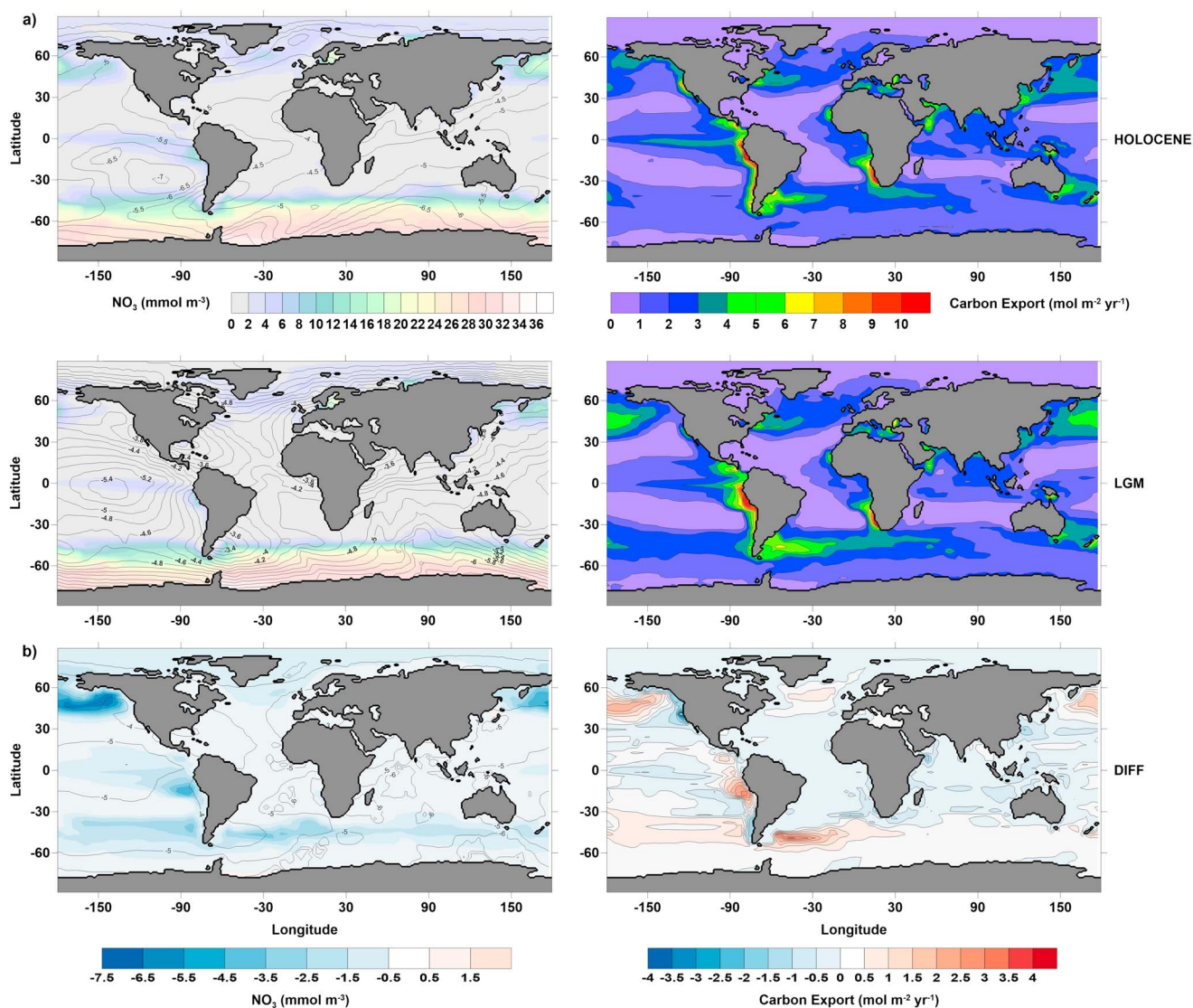


Figure 3. (a) left column: Holocene and LGM surface nitrate concentrations (mmol m^{-3}) in color superposed with contour lines showing surface iron fluxes ($\text{kg m}^{-2} \text{yr}^{-1}$) in powers of 10. (right column) Holocene and LGM annual carbon export ($\text{mol C m}^{-2} \text{yr}^{-1}$) at 100 m depth. (b) Same as Figure 3a but for the LGM-Holocene difference.

difference has been attributed to a more efficient biological pump due to increased LGM iron fertilization of the subantarctic SO [Watson *et al.*, 2000; Kohfeld *et al.*, 2005; Jaccard *et al.*, 2013], whereby the solubility pump drawdown may have been compensated to a large degree by a decreased terrestrial biosphere and increased ocean salinity [Sigman and Boyle, 2000]. However, in our 500 year PISCES simulation atmospheric $p\text{CO}_2$ was only reduced by <10 ppmv between the LGM and the Holocene, due to the enhanced dust-induced carbon sequestration via the soft tissue pump (although there is an additional long-term effect discussed below). The small change in atmospheric $p\text{CO}_2$, despite larger carbon export and overall greater absolute dust fluxes in most regions than in previous climate model simulations, suggests that enhanced global iron deposition only had a limited influence on atmospheric $p\text{CO}_2$ levels over centennial timescales. This is likely due to the role of other iron sources in the high-latitude SO [Tagliabue *et al.*, 2014] and/or reduced CO_2 drawdown at low latitudes (see discussion of Figure 4b). Our results are similar to other ocean biogeochemical model simulations that estimate low atmospheric $p\text{CO}_2$ reductions (8–15 ppm) due to increased LGM dust loads [Bopp *et al.*, 2003; Parekh *et al.*, 2006; Tagliabue *et al.*, 2009], although other box model studies still attribute a more substantial role (~ 35 ppm) to iron fertilization [Hain *et al.*, 2010].

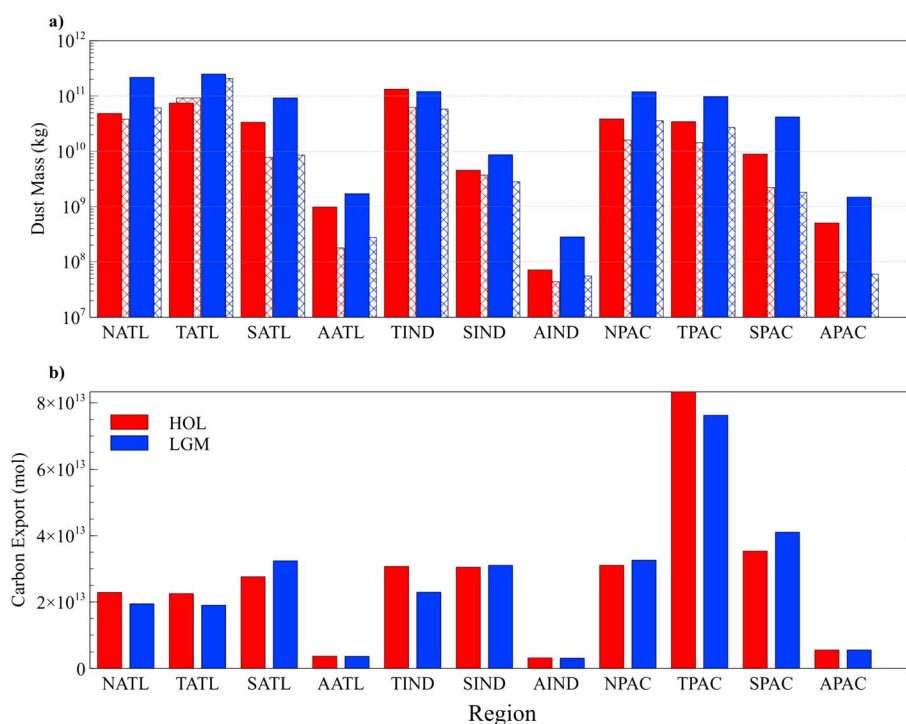


Figure 4. Deposited dust masses and carbon export integrated over ocean basins (ATL-Atlantic, IND-Indian, PAC-Pacific; North is latitude > 30 , Tropical is $-30 > \text{latitude} > 30$, South is $-60 < \text{latitude} < -30$, Antarctic is latitude < -60) for Holocene and LGM conditions. The crossed bars in the dust plot represent the model ensemble median. The North Atlantic (NATL) includes the Mediterranean, and the Tropical Indian Ocean (TIND) includes the Red Sea and the Persian Gulf.

Figure 4 shows dust fluxes integrated over 1 year for the interpolation and the four climate models' (CCSM, MIROC, MIROC-ESM, and MRI) ensemble median, as well as the simulated (PISCES) ocean carbon export fluxes by ocean basin. Under Holocene conditions, the climate model median is within a factor 2 of the interpolated dust fluxes in most regions (Figure 4a). However, the SO and the North Pacific dust deposition are strongly underestimated by the climate models, which is significant since these are the HNLC regions that are most likely to respond to dust variations. Under LGM conditions, the models tend to underestimate dust increases in most regions, notably the North Atlantic, which in our interpolation receives a very large additional dust input from North American sources. Generally, the models tend to perform better in low than in high latitudes [Lambert *et al.*, 2013].

Stronger glacial sources in Australia and New Zealand resulted in increased LGM dust deposition in the South Pacific. But despite the larger size of the ocean basin, the South Pacific only received about half as much dust as the South Atlantic. This suggests that Australian and New Zealand sources produced a lower absolute amount of dust than South American sources.

Basin changes in the impact of dust iron on carbon export between the Holocene and the LGM depend on the role of iron limitation in each region and macronutrient transport by ocean currents. The main source of macronutrients for biological productivity in low latitudes is thought to be intermediate depth waters originating from the SO surface layers [Toggweiler *et al.*, 1991; Sarmiento *et al.*, 2004; Sigman *et al.*, 2010]. Thus, any change in macronutrient concentrations of the subantarctic ocean will be conveyed to other ocean regions [Boyle, 1988; Palter *et al.*, 2005; Tagliabue *et al.*, 2008, 2014]. In PISCES, the subantarctic south Atlantic and south Pacific Oceans are iron limited and we find additional carbon export due to the greater LGM dust supply (Figure 4b). Conversely, non-iron-limited regions such as the tropical oceans show a reduction of carbon export. More efficient biological carbon sequestration in iron-limited subantarctic regions reduces nutrient concentrations in the SO surface waters. Then, as expected, these local nutrient deficits are transported at intermediate depths toward low latitudes, reducing carbon export and thereby CO_2 drawdown when these waters upwell into tropical nitrate-limited regions [Matsumoto *et al.*, 2002;

Louber, 2004; Tagliabue et al., 2014]. Any LGM reduction in subantarctic mode water production was not simulated in our simulations, but would exacerbate this effect [Sigman et al., 2010]. Thus, even if dust iron content and solubility had been higher during the LGM, it is likely that any greater carbon export in the SO would have been partially compensated for by reduced tropical carbon export. In PISCES, increased LGM dust deposition in the Antarctic SO was not sufficient to elevate iron-limited growth rates (as was the case in other regions), causing little increase in Antarctic SO carbon export (Figure 4b and SI Figure S8). Antarctic SO changes in marine productivity between glacial and interglacial climates [Kohfeld et al., 2013] may therefore have been largely driven by other factors, such as changes in ocean physics and/or sea ice extent.

To estimate the complete iron fertilization effect at millennial timescales (not possible by design with PISCES) we conducted simulations using the DCESS Earth System Model of Intermediate Complexity [Shaffer et al., 2008]. The high-latitude phytoplankton growth rate limitation factor in the DCESS model was adjusted to mirror the ~20% increase in SO export production found in the PISCES LGM simulation due to dust-driven iron fertilization (Figure 4b). When forced by these enhanced growth rates, the DCESS model simulations showed $p\text{CO}_2$ reductions of 8.3 ppm from the standard, preindustrial simulation after 500 years (in good agreement with PISCES model results) and 10.3, 15.3, 17.7, and 19.8 ppm after 1000, 10,000, 25,000, and 50,000 years, respectively. The long-term $p\text{CO}_2$ reductions are due to enhanced organic carbon burial in ocean sediments and carbonate compensation that draws down the ocean inventory of dissolved inorganic carbon and thereby $p\text{CO}_2$. Enhanced burial also draws down the ocean inventory of phosphate, the master nutrient of this model. This leads to a slow overall production decrease but with retained enhancement of high-latitude new production (SI Figure S9).

4. Conclusions

We present here two interpolated global data sets of dust fluxes for both average Holocene and LGM climatic conditions, based on measurements in various paleoclimatic archives. A comparison with PMIP2 and PMIP3 model outputs suggests that most climate models seem to put too much emphasis on the North African sources and underestimate sources in Asia and the Americas. In particular, models underestimate dust deposition in HNLC regions.

A global ocean biogeochemical model forced with the interpolated dust fields simulated a small global reaction of the carbon cycle to strongly increased (LGM) ocean dust deposition. The LGM-Holocene carbon export changes display a clear difference between high and low latitudes, with the iron-limited polar oceans and the nitrate-limited tropical oceans showing a large increase and decrease, respectively. This tropical ocean decrease kept the global effect of iron fertilization on atmospheric $p\text{CO}_2$ below 10 ppmv over centennial timescale. A supplementary Earth System Model simulation showed an additional atmospheric $p\text{CO}_2$ drawdown of ~10 ppm on multimillennial timescales due mainly to enhanced ocean carbon burial. Thus, predictions from ocean biogeochemistry models are underestimates of the millennial-scale impact of iron fertilization on atmospheric CO_2 . Based on our results, the LGM atmospheric $p\text{CO}_2$ was reduced by ~20 ppm due to enhanced dust loads and the associated iron fertilization of the oceans. Hence, it is likely that besides ocean stratification and iron fertilization, additional processes must be significant contributors to low glacial CO_2 levels.

Acknowledgments

The Dust Flux data set is available on NOAA's paleoclimate data server and the PANGAEA data server (doi:10.1594/PANGAEA.847983). We thank two anonymous reviewers for their time and help in improving this manuscript. We thank Garritt L. Page for helpful suggestions on statistical aspects. F. Lambert acknowledges support by Projects CONICYT 15110009, 1151427, and NC120066. G. Shaffer was supported by FONDECYT grant 1120040. This work made use of the facilities of N8 HPC provided and funded by the N8 consortium and EPSRC (grant EP/K000225/1). The Centre is coordinated by the Universities of Leeds and Manchester.

The Editor thanks two anonymous reviewers for their assistance in evaluating this paper.

References

- Albani, S., N. M. Mahowald, A. T. Perry, R. A. Scanza, C. S. Zender, N. G. Heavens, V. Maggi, J. F. Kok, and B. L. Otto-Bliesner (2014), Improved dust representation in the Community Atmosphere Model, *J. Adv. Model. Earth Syst.*, 6(3), 541–570, doi:10.1002/2013MS000279.
- Aleinikoff, J. N., D. R. Muhs, I. Bettis, E. Arthur, W. C. Johnson, C. M. Fanning, and R. Benton (2008), Isotopic evidence for the diversity of late Quaternary loess in Nebraska: Glaciogenic and nonglaciogenic sources, *Geol. Soc. Am. Bull.*, 120(11–12), 1362–1377.
- Anderson, R. F., S. Barker, M. Fleisher, R. Gersonde, S. L. Goldstein, G. Kuhn, P. G. Mortyn, K. Pahnke, and J. P. Sachs (2014), Biological response to millennial variability of dust and nutrient supply in the Subantarctic South Atlantic Ocean, *Philos. Trans. A Math. Phys. Eng. Sci.*, 372(2019), 20130054, doi:10.1098/rsta.2013.0054.
- Biscaye, P. E., F. E. Grousset, M. Revel, S. Van der Gaast, G. A. Zielinski, A. Vaars, and G. Kukla (1997), Asian provenance of glacial dust (stage 2) in the Greenland Ice Sheet Project 2 Ice Core, Summit, Greenland, *J. Geophys. Res.*, 102(C12), 26,765–26,781, doi:10.1029/97JC01249.
- Blain, S., S. Bonnet, and C. Guieu (2008), Dissolved iron distribution in the tropical and sub tropical South Eastern Pacific, *Biogeosciences*, 5, 269–280.
- Bopp, L., K. E. Kohfeld, and C. Le Quéré (2003), Dust impact on marine biota and atmospheric CO_2 during glacial periods, *Paleoceanography*, 18(2), 1046, doi:10.1029/2002PA000810.

- Boyd, P. W., et al. (2000), A mesoscale phytoplankton bloom in the polar Southern Ocean stimulated by iron fertilization, *Nature*, 407(6805), 695–702, doi:10.1038/35037500.
- Boyd, P. W., et al. (2007), Mesoscale iron enrichment experiments 1993–2005: Synthesis and future directions, *Science*, 315(5812), 612–617, doi:10.1126/science.1131669.
- Boyle, E. A. (1988), Vertical oceanic nutrient fractionation and glacial/interglacial CO₂ cycles, *Nature*, 331(6151), 55–56, doi:10.1038/331055a0.
- Bristow, C. S., K. A. Hudson-Edwards, and A. Chappell (2010), Fertilizing the Amazon and equatorial Atlantic with West African dust, *Geophys. Res. Lett.*, 37, L14807, doi:10.1029/2010GL043486.
- Burton, G. R., K. J. R. Rosman, J.-P. Candelone, L. J. Burn, C. F. Boutron, and S. Hong (2007), The impact of climatic conditions on Pb and Sr isotopic ratios found in Greenland ice, 7–150 ky BP, *Earth Planet. Sci. Lett.*, 259(3–4), 557–566, doi:10.1016/j.epsl.2007.05.015.
- Coale, K. H., et al. (1996), A massive phytoplankton bloom induced by an ecosystem-scale iron fertilization experiment in the equatorial Pacific Ocean, *Nature*, 383(6600), 495–501, doi:10.1038/383495a0.
- Cressie, N. (1991), *Statistics for Spatial Data*, John Wiley, New York.
- De Baar, H. J. W. (2005), Synthesis of iron fertilization experiments: From the Iron Age in the Age of Enlightenment, *J. Geophys. Res.*, 110, C09S16, doi:10.1029/2004JC002601.
- Fischer, H., M. L. Siggaard-Andersen, U. Ruth, R. Röthlisberger, and E. W. Wolff (2007), Glacial/Interglacial changes in mineral dust and sea-salt records in polar ice cores: Sources, transport, and deposition, *Rev. Geophys.*, 45, RG1002, doi:10.1029/2005RG000192.
- Fischer, H., et al. (2010), The role of Southern Ocean processes in orbital and millennial CO₂ variations—A synthesis, *Quat. Sci. Rev.*, 29(1–2), 193–205, doi:10.1016/j.quascirev.2009.06.007.
- Francois, R., M. Altabet, E. Yu, D. Sigman, M. Bacon, M. Frank, G. Bohrmann, G. Bareille, and L. Labeyrie (1997), Contribution of Southern Ocean surface-water stratification to low atmospheric CO₂ concentrations during the last glacial period, *Nature*, 389, 929–935.
- Hain, M. P., D. M. Sigman, and G. H. Haug (2010), Carbon dioxide effects of Antarctic stratification, North Atlantic Intermediate Water formation, and subantarctic nutrient drawdown during the last ice age: Diagnosis and synthesis in a geochemical box model, *Global Biogeochem. Cycles*, 24, GB4023, doi:10.1029/2010GB003790.
- Hain, M. P., D. M. Sigman, and G. H. Haug (2014), *Treatise on Geochemistry*, Elsevier, Amsterdam.
- Hansson, M. E. (1994), The Renland ice core. A Northern Hemisphere record of aerosol composition over 120,000 years, *Tellus B*, 46(5), doi:10.3402/tellusb.v46i5.15813.
- Huneeeu, N., L. Gallardo, and J. A. Rutllant (2006), Offshore transport episodes of anthropogenic sulfur in northern Chile: Potential impact on the stratocumulus cloud deck, *Geophys. Res. Lett.*, 33, L19819, doi:10.1029/2006GL026921.
- Huneeeu, N., et al. (2011), Global dust model intercomparison in AeroCom phase I, *Atmos. Chem. Phys.*, 11(15), 7781–7816, doi:10.5194/acp-11-7781-2011.
- Jaccard, S. L., C. T. Hayes, A. Martínez-García, D. A. Hodell, R. F. Anderson, D. M. Sigman, and G. H. Haug (2013), Two modes of change in Southern Ocean productivity over the past million years, *Science*, 339(6126), 1419–1423, doi:10.1126/science.1227545.
- Kohfeld, K. E., and S. P. Harrison (2001), DIRTMAP: The geological record of dust, *Earth Sci. Rev.*, 54(1–3), 81–114, doi:10.1016/S0012-8252(01)00042-3.
- Kohfeld, K. E., C. Le Quéré, S. P. Harrison, and R. F. Anderson (2005), Role of marine biology in glacial-interglacial CO₂ cycles, *Science*, 308(5718), 74–78, doi:10.1126/science.1105375.
- Kohfeld, K. E., R. M. Graham, A. M. de Boer, L. C. Sime, E. W. Wolff, C. Le Quéré, and L. Bopp (2013), Southern Hemisphere westerly wind changes during the Last Glacial Maximum: Paleo-data synthesis, *Quat. Sci. Rev.*, 68, 76–95, doi:10.1016/j.quascirev.2013.01.017.
- Kylander, M. E., R. Bindler, A. M. Cortizas, K. Gallagher, C.-M. Mörtz, and S. Rauch (2013), A novel geochemical approach to paleorecords of dust deposition and effective humidity: 8500 years of peat accumulation at Store Mosse (the “Great Bog”), Sweden, *Quat. Sci. Rev.*, 69, 69–82, doi:10.1016/j.quascirev.2013.02.010.
- Lambert, F., B. Delmonte, J. Petit, M. Bigler, P. Kaufmann, M. Hutterli, T. Stocker, U. Ruth, J. Steffensen, and V. Maggi (2008), Dust-climate couplings over the past 800,000 years from the EPICA Dome C ice core, *Nature*, 452(7187), 616–619, doi:10.1038/nature06763.
- Lambert, F., M. Bigler, J. Steffensen, M. Hutterli, and H. Fischer (2012), Centennial mineral dust variability in high-resolution ice core data from Dome C, Antarctica, *Clim. Past*, 8(2), 609–623, doi:10.5194/cp-8-609-2012.
- Lambert, F., J.-S. Kug, R. J. Park, N. Mahowald, G. Winckler, A. Abe-Ouchi, R. Oishi, T. Takemura, and J.-H. Lee (2013), The role of mineral-dust aerosols in polar temperature amplification, *Nat. Clim. Change*, 3(5), 487–491, doi:10.1038/nclimate1785.
- Lamy, F., R. Gersonde, G. Winckler, O. Esper, A. Jaeschke, G. Kuhn, J. Ullermann, A. Martínez-García, F. Lambert, and R. Kilian (2014), Increased dust deposition in the Pacific Southern Ocean during glacial periods, *Science*, 343(6169), 403–407, doi:10.1126/science.1245424.
- Lohmann, U., and J. Feichter (2005), Global indirect aerosol effects: A review, *Atmos. Chem. Phys.*, 5(3), 715–737, doi:10.5194/acp-5-715-2005.
- Loubere, P. (2004), Export fluxes of calcite in the eastern equatorial Pacific from the Last Glacial Maximum to present, *Paleoceanography*, 19, PA2018, doi:10.1029/2003PA000986.
- Maher, B. A., J. M. Prospero, D. Mackie, D. Gaiero, P. P. Hesse, and Y. Balkanski (2010), Global connections between aeolian dust, climate and ocean biogeochemistry at the present day and at the last glacial maximum, *Earth Sci. Rev.*, 99(1–2), 61–97, doi:10.1016/j.earscirev.2009.12.001.
- Mahowald, N. (2011), Aerosol indirect effect on biogeochemical cycles and climate, *Science*, 334(6057), 794–796, doi:10.1126/science.1207374.
- Mahowald, N., K. Kohfeld, M. Hansson, Y. Balkanski, S. P. Harrison, I. C. Prentice, M. Schulz, and H. Rodhe (1999), Dust sources and deposition during the last glacial maximum and current climate: A comparison of model results with paleodata from ice cores and marine sediments, *J. Geophys. Res.*, 104(D13), 15,895–15,916, doi:10.1029/1999JD900084.
- Mahowald, N. M., D. R. Muhs, S. Levis, P. J. Rasch, M. Yoshioka, C. S. Zender, and C. Luo (2006), Change in atmospheric mineral aerosols in response to climate: Last glacial period, preindustrial, modern, and doubled carbon dioxide climates, *J. Geophys. Res.*, 111, D10202, doi:10.1029/2005JD006653.
- Martin, J. H. (1990), Glacial-interglacial CO₂ change: The iron hypothesis, *Paleoceanography*, 5(1), 1–13, doi:10.1029/PA0051001p00001.
- Martin, J. H., and S. E. Fitzwater (1988), Iron deficiency limits phytoplankton growth in the north-east Pacific subarctic, *Nature*, 331(6154), 341–343, doi:10.1038/331341a0.
- Martin, J. H., R. M. Gordon, and S. E. Fitzwater (1990), Iron in Antarctic waters, *Nature*, 345(6271), 156–158, doi:10.1038/345156a0.
- Martin, J. H., R. M. Gordon, and S. E. Fitzwater (1991), The case for iron, *Limnol. Oceanogr.*, 36(8), 1793–1802.
- Martínez-Botí, M. A., G. Marino, G. L. Foster, P. Ziveri, M. J. Henehan, J. W. B. Rae, P. G. Mortyn, and D. Vance (2015), Boron isotope evidence for oceanic carbon dioxide leakage during the last deglaciation, *Nature*, 518(7538), 219–222, doi:10.1038/nature14155.
- Martínez-García, A., A. Rosell-Melé, W. Geibert, R. Gersonde, P. Masqué, V. Gaspari, and C. Barbante (2009), Links between iron supply, marine productivity, sea surface temperature, and CO₂ over the last 1.1 Ma, *Paleoceanography*, 24, PA1207, doi:10.1029/2008PA001657.

- Martínez-García, A., A. Rosell-Melé, S. L. Jaccard, W. Geibert, D. M. Sigman, and G. H. Haug (2011), Southern Ocean dust–climate coupling over the past four million years, *Nature*, *476*(7360), 312–315, doi:10.1038/nature10310.
- Martínez-García, A., D. M. Sigman, H. Ren, R. F. Anderson, M. Straub, D. A. Hodell, S. L. Jaccard, T. I. Eglinton, and G. H. Haug (2014), Iron fertilization of the subantarctic ocean during the last ice age, *Science*, *343*(6177), 1347–1350, doi:10.1126/science.1246848.
- Matsumoto, K., J. L. Sarmiento, and M. A. Brzezinski (2002), Silicic acid leakage from the Southern Ocean: A possible explanation for glacial atmospheric $p\text{CO}_2$, *Global Biogeochem. Cycles*, *16*(3), 1031, doi:10.1029/2001GB001442.
- Mills, M. M., C. Ridame, M. Davey, J. La Roche, and R. J. Geider (2004), Iron and phosphorus co-limit nitrogen fixation in the eastern tropical North Atlantic, *Nature*, *429*(6989), 292–294, doi:10.1038/nature02550.
- Nielsdóttir, M. C., C. M. Moore, R. Sanders, D. J. Hinz, and E. P. Achterberg (2009), Iron limitation of the postbloom phytoplankton communities in the Iceland Basin, *Global Biogeochem. Cycles*, *23*, GB3001, doi:10.1029/2008GB003410.
- Palter, J. B., M. S. Lozier, and R. T. Barber (2005), The effect of advection on the nutrient reservoir in the North Atlantic subtropical gyre, *Nature*, *437*(7059), 687–92, doi:10.1038/nature03969.
- Parekh, P., S. Dutkiewicz, M. J. Follows, and T. Ito (2006), Atmospheric carbon dioxide in a less dusty world, *Geophys. Res. Lett.*, *33*, L03610, doi:10.1029/2005GL025098.
- Ridgwell, A. J. (2003), Implications of the glacial CO_2 “iron hypothesis” for Quaternary climate change, *Geochem. Geophys. Geosyst.*, *4*(9), 1076, doi:10.1029/2003GC000563.
- Röthlisberger, R., M. Bigler, E. W. Wolff, F. Joos, E. Monnin, and M. A. Hutterli (2004), Ice core evidence for the extent of past atmospheric CO_2 change due to iron fertilisation, *Geophys. Res. Lett.*, *31*, L16207, doi:10.1029/2004GL020338.
- Ruth, U., D. Wagenbach, J. P. Steffensen, and M. Bigler (2003), Continuous record of microparticle concentration and size distribution in the central Greenland NGRIP ice core during the last glacial period, *J. Geophys. Res.*, *108*(D3), 4098, doi:10.1029/2002JD002376.
- Saide, P. E., G. R. Carmichael, S. N. Spak, P. Minnis, and J. K. Ayers (2012), Improving aerosol distributions below clouds by assimilating satellite-retrieved cloud droplet number, *Proc. Natl. Acad. Sci. U.S.A.*, *109*(30), 11,939–11,943, doi:10.1073/pnas.1205877109.
- Sarmiento, J. L., N. Gruber, M. A. Brzezinski, and J. P. Dunne (2004), High-latitude controls of thermocline nutrients and low latitude biological productivity, *Nature*, *427*(6969), 56–60, doi:10.1038/nature02127.
- Sassen, K., P. J. Demott, J. M. Prospero, and M. R. Poellot (2003), Saharan dust storms and indirect aerosol effects on clouds: CRYSTAL-FACE results, *Geophys. Res. Lett.*, *30*(12), 1633, doi:10.1029/2003GL017371.
- Schroth, A. W., J. Crusius, E. R. Sholkovitz, and B. C. Bostick (2009), Iron solubility driven by speciation in dust sources to the ocean, *Nat. Geosci.*, *2*(5), 337–340, doi:10.1038/ngeo501.
- Shaffer, G., S. Malskær Olsen, and J. O. Pepke Pedersen (2008), Presentation, calibration and validation of the low-order, DCESS Earth System Model (Version 1), *Geosci. Model Dev.*, *1*(1), 17–51, doi:10.5194/gmd-1-17-2008.
- Sigman, D. M., and E. A. Boyle (2000), Glacial/interglacial variations in atmospheric carbon dioxide, *Nature*, *407*(6806), 859–869, doi:10.1038/35038000.
- Sigman, D. M., M. P. Hain, and G. H. Haug (2010), The polar ocean and glacial cycles in atmospheric CO_2 concentration, *Nature*, *466*(7302), 47–55, doi:10.1038/nature09149.
- Smetacek, V., et al. (2012), Deep carbon export from a Southern Ocean iron-fertilized diatom bloom, *Nature*, *487*(7407), 313–9, doi:10.1038/nature11229.
- Sokolik, I., D. Winker, G. Bergametti, D. A. Gillette, G. Carmichael, Y. J. Kaufman, L. Gomes, L. Schuetz, and J. E. Penner (2001), Introduction to special section: Outstanding problems in quantifying the radiative impacts of mineral dust, *J. Geophys. Res.*, *106*(D16), 18,015–18,027, doi:10.1029/2000JD900498.
- Steffensen, J. P. (1997), The size distribution of microparticles from selected segments of the Greenland Ice Core Project ice core representing different climatic periods, *J. Geophys. Res.*, *102*(C12), 26,755–26,763, doi:10.1029/97JC01490.
- Svensson, A., P. E. Biscaye, and F. E. Grousset (2000), Characterization of late glacial continental dust in the Greenland Ice Core Project ice core, *J. Geophys. Res.*, *105*(D4), 4637–4656, doi:10.1029/1999JD901093.
- Tagliabue, A., L. Bopp, and O. Aumont (2008), Ocean biogeochemistry exhibits contrasting responses to a large scale reduction in dust deposition, *Biogeosciences*, *5*(1), 11–24, doi:10.5194/bg-5-11-2008.
- Tagliabue, A., L. Bopp, D. Roche, N. Bouttes, J. Dutay, R. Alkama, M. Kageyama, E. Michel, and D. Paillard (2009), Quantifying the roles of ocean circulation and biogeochemistry in governing ocean carbon-13 and atmospheric carbon dioxide at the last glacial maximum, *Clim. Past*, *5*, 695–706.
- Tagliabue, A., O. Aumont, and L. Bopp (2014), The impact of different external sources of iron on the global carbon cycle, *Geophys. Res. Lett.*, *41*, 920–926, doi:10.1002/2013GL059059.
- Takemura, T., M. Egashira, K. Matsuzawa, H. Ichijo, R. O’ishi, and A. Abe-Ouchi (2009), A simulation of the global distribution and radiative forcing of soil dust aerosols at the Last Glacial Maximum, *Atmos. Chem. Phys.*, *9*(9), 3061–3073, doi:10.5194/acp-9-3061-2009.
- Tegen, I. (2003), Modeling the mineral dust aerosol cycle in the climate system, *Quat. Sci. Rev.*, *22*(18–19), 1821–1834, doi:10.1016/S0277-3791(03)00163-X.
- Tegen, I., A. A. Lacis, and I. Fung (1996), The influence on climate forcing of mineral aerosols from disturbed soils, *Nature*, *380*(6573), 419–422, doi:10.1038/380419a0.
- Toggweiler, J. R., K. Dixon, and W. S. Broecker (1991), The Peru upwelling and the ventilation of the south Pacific thermocline, *J. Geophys. Res.*, *96*(C11), 20,467–20,497, doi:10.1029/91JC02063.
- Watanabe, S., et al. (2011), MIROC-ESM 2010: Model description and basic results of CMIP5-20c3m experiments, *Geosci. Model Dev.*, *4*(4), 845–872, doi:10.5194/gmd-4-845-2011.
- Watson, A. J., D. C. Bakker, A. J. Ridgwell, P. W. Boyd, and C. S. Law (2000), Effect of iron supply on Southern Ocean CO_2 uptake and implications for glacial atmospheric CO_2 , *Nature*, *407*(6805), 730–733, doi:10.1038/35037561.
- Werner, M., I. Tegen, S. P. Harrison, K. E. Kohfeld, I. C. Prentice, Y. Balkanski, H. Rodhe, and C. Roelandt (2002), Seasonal and interannual variability of the mineral dust cycle under present and glacial climate conditions, *J. Geophys. Res.*, *107*(D24), 4744, doi:10.1029/2002JD002365.
- Winckler, G., R. F. Anderson, M. Q. Fleisher, D. McGee, and N. Mahowald (2008), Covariant glacial-interglacial dust fluxes in the equatorial Pacific and Antarctica, *Science*, *320*(5872), 93–96, doi:10.1126/science.1150595.
- Yukimoto, S., et al. (2012), A New global climate model of the meteorological research institute: MRI-CGCM3, *J. Meteorol. Soc. Jpn.*, *90A*, 23–64, doi:10.2151/jmsj.2012-A02.
- Zickfeld, K., et al. (2013), Long-term climate change commitment and reversibility: An EMIC intercomparison, *J. Clim.*, *26*(16), 5782–5809, doi:10.1175/JCLI-D-12-00584.1.